

This article was downloaded by:

On: 21 January 2011

Access details: *Access Details: Free Access*

Publisher *Taylor & Francis*

Informa Ltd Registered in England and Wales Registered Number: 1072954 Registered office: Mortimer House, 37-41 Mortimer Street, London W1T 3JH, UK



## The Journal of Adhesion

Publication details, including instructions for authors and subscription information:

<http://www.informaworld.com/smpp/title~content=t713453635>

### Ultrasonic Guided Waves Scattering Effects From Defects in Adhesively Bonded Lap Joints Using Pitch and Catch and Pulse-Echo Techniques

M. J. Santos<sup>a</sup>; J. Perdigão<sup>a</sup>; P. Faia<sup>a</sup>

<sup>a</sup> Institute of Science and Materials Engineering, Department of Electrical and Computers Engineering, University of Coimbra, Portugal

**To cite this Article** Santos, M. J. , Perdigão, J. and Faia, P.(2008) 'Ultrasonic Guided Waves Scattering Effects From Defects in Adhesively Bonded Lap Joints Using Pitch and Catch and Pulse-Echo Techniques', *The Journal of Adhesion*, 84: 5, 421 – 438

**To link to this Article:** DOI: 10.1080/00218460802089262

**URL:** <http://dx.doi.org/10.1080/00218460802089262>

PLEASE SCROLL DOWN FOR ARTICLE

Full terms and conditions of use: <http://www.informaworld.com/terms-and-conditions-of-access.pdf>

This article may be used for research, teaching and private study purposes. Any substantial or systematic reproduction, re-distribution, re-selling, loan or sub-licensing, systematic supply or distribution in any form to anyone is expressly forbidden.

The publisher does not give any warranty express or implied or make any representation that the contents will be complete or accurate or up to date. The accuracy of any instructions, formulae and drug doses should be independently verified with primary sources. The publisher shall not be liable for any loss, actions, claims, proceedings, demand or costs or damages whatsoever or howsoever caused arising directly or indirectly in connection with or arising out of the use of this material.

## Ultrasonic Guided Waves Scattering Effects From Defects in Adhesively Bonded Lap Joints Using Pitch and Catch and Pulse-Echo Techniques

M. J. Santos, J. Perdigão, and P. Faia

Institute of Science and Materials Engineering, Department of Electrical and Computers Engineering, University of Coimbra, Portugal

*In this article a method to evaluate defect dimensions in adhesively bonded lap joints based on the measurement of scattering effects of ultrasonic guided waves is presented. A simplified theoretical model is proposed which was initially tested in plates with through holes. The experimental results obtained using both pitch-and-catch and pulse-echo techniques for 500 kHz and 1 MHz frequencies confirm the validity of this model. To evaluate the lap joint defects, a set of samples with artificial defects were manufactured and the form and dimensions were confirmed using C-scan ultrasonic images. With the same methodology used in through-hole analysis, scattering effects of defects were measured. The results obtained with the pitch-and-catch technique with 1 MHz transducers allow us to say that an estimate of defect dimensions could be done by using the proposed model with reasonable accuracy and according with the predictions.*

**Keywords:** Adhesively bonded lap joint; Defect sizing; Pitch-and-catch; Pulse-echo; Scattering; Ultrasonic guided waves

### 1. INTRODUCTION

Adhesive bonding has been used for sometime with success in industrial fabrication processes, namely, in aerospace and automotive industries. One of the advantages, when compared with other traditional techniques such as bolting, riveting, or spot welding, is the fact that unavoidable stress between the parts could be transmitted more uniformly. Besides, bonding gives also a smoother appearance

Received 1 August 2007; in final form 21 February 2008.

Address correspondence to M. J. Santos, Faculdade de Ciências e Tecnologia, Departamento de Engenharia, Electrotechnica e de Computadores, Universidade de Coimbra, Coimbra 3030-290, Portugal. E-mail: marioj@deec.uc.pt

and light weight to the final assembly and the ability to join different materials in complex shape structures.

Adhesive bond defects can be divided into three different types [1]: adhesive defects that are related to the weak bond between the adhesive and the adherend, cohesive defects related to mechanical properties of the adhesive, and gross defects such as cracking, disbonding, porosity, and voids. These gross defects, especially voids, are the simplest forms of defects to detect and size using ultrasonic non-destructive testing.

There is a large number of papers in the literature dedicated to ultrasonic non-destructive testing of adhesively bonded joints [1–11]. The classical pulse-echo and transmission techniques have been used for the detection of flaws in the joints [1,2] and to evaluate the integrity of the joint under test [3]. Although the latter technique is effective in detecting disbondings, it needs access to both faces of the material under test which, sometimes, is not feasible. So, the most suitable of the classical techniques is sometimes pulse-echo, which allows inspection from only one side.

To avoid the need for a liquid or gelatinous couplant between the transducer and test structure, some authors use air-coupling in the study of diffusion bonds [5] and to obtain C-scan images of defects in bonded aluminium lap joints [6].

A combination of different ultrasonic techniques that use longitudinal waves and shear waves with standard damped transducers and high power ultrasonic inspection with electro-magnetic acoustic transducers (EMAT) is used, with promising results, to detect the “kissing” bonds in adhesive joints [7].

Another type of technique often used is based on spectral analysis of the ultrasonic signal that comes from the bonded specimen [8]. Some practical applications were developed for the automotive industry applying this technique and analysing the first mode ultrasonic resonance [9,10]. Also based on this approach, the Fokker bond tester [11] is perhaps the most widely used commercial equipment: it compares the through-thickness resonance of a single sheet with the resonance of the joint. The frequency shift between spectra is usually correlated with the bond condition.

Generally, sizing of voids and disbonds is done using perpendicular incidence associated with conventional point by point techniques, which is very time-consuming since the transducer needs to scan each point of the structure to be tested. The use of ultrasonic guided waves is, potentially, a very attractive solution when large structural tests are demanded, since they can be excited at one point and propagated over considerable distances with low attenuation, which results in

considerable time saving. With the transmission technique, information about the line between transmitter and receiver is obtained. With pulse-echo the obtained information is about the line between transmitter and target.

Several authors have studied the propagation of guided waves in adhesively bonded lap joints and the influence of bond conditions on wave parameters [12–22]. In some of these studies, laser ultrasonic techniques were used to obtain the degree of aging [13] or detection of large disbonds [14,15]. Kissing bonds, which are invisible to longitudinal waves when subjected to high compressive strength, can be detected by the proper Lamb wave mode selection [16]. Other contributions have been made to the understanding of transmission of guided waves in lap joints with the help of analytical models [17,18], finite elements [19], wavelet transforms [20], or artificial neural networks [21].

The present work is motivated by the necessity for quantitative analysis of defects in adhesively bonded lap joints using guided waves. Two different setups were used: immersion pitch-and-catch and pulse-echo. In a first set of experiments, aluminium plates with through holes were analysed and experimental results compared with theoretical ones obtained with a simplified scattering model that considers, as an approximation, the incident propagation mode with exclusively out-of-plane displacement. The same methodology was used to analyse lap joints with artificial defects.

## 2. BACKGROUND

### 2.1. Propagation of Ultrasonic Guided Waves in Multilayered Systems

The propagation of guided waves in a bonded lap joint can be modelled as a generic propagation problem in a multilayered structure. In this particular case, three layers (two adherends and the adhesive) are considered. The study of this propagation problem may be developed from matrix formulations which describe elastic waves in layered media. The transfer matrix method is certainly the most important technique employing these matrix formulations [23]. This technique combines the theory of the dynamics of the continuum within each layer with the conditions for the interaction at the interfaces between layers. For each layer, a set of four equations relating the boundary conditions at the first interface with those at the last interface is considered. In the process, the equations for the intermediate interfaces are eliminated, so that the fields in all of the layers of the structure are

described solely in terms of the external boundary conditions. The modal solution can be obtained by solving the resulting matrix system.

An important problem of the transfer matrix method is the instability of the solution when layers of large thickness are presented and high frequencies are considered. This is known as the “large  $fd$  problem” [23].

An alternative to the transfer matrix method that could be used to avoid the large  $fd$  problem is the global matrix method. In this technique, a large single matrix is assembled, consisting of all of the equations for all the layers. The method has the additional advantage that the same matrix may be used for all categories of the solution, either response or modal, vacuum or solid half-spaces, real or complex plate wavenumber. The disadvantage of the method is that the global matrix may be large and, therefore, reaching the solution may be relatively slow.

Modal solution, which can be obtained by both methods, gives rise to the so-called dispersion curves, which represent the allowed propagation guided modes in a structure as a function of the frequency. Each of these modes has a particular phase velocity, group velocity, and particle displacements for a given frequency and can be seen as a wave packet.

In the original approach to the ultrasonic guided wave propagation problem, only true modes (waves travelling without decay) were analysed. When a damping medium or decay of the guided wave due to energy leak in an embedded medium is considered, the attenuation can be modelled in several ways. A convenient and popular approach is based in the Kelvin-Voigt viscoelastic model, which considers a complex propagation wavenumber. The real part of the wavenumber describes the propagation of the wave and the imaginary part the attenuation [24].

## 2.2. Scattering of Ultrasonic Waves from Circular Obstacles

The application of guided waves for the study of lap joints has been reported by some authors [12,19,21,25]. These papers deal with the theoretical and experimental analysis of wave propagation in the bond line and also with the detection of existing defects. The quantitative analysis (detection and sizing) of the scattering effects of existing voids studied in this work is based on the scattering effects of a through-hole in a plate. This problem has been studied by several authors [22,26–30]. One of these studies [22] uses a simplified model, based on the perturbation of the field caused by a cylindrical obstacle, perpendicular to the plate, in the presence of an incident out-of-plane field. In this

approach, using a cylindrical coordinates system  $(r, \theta, z)$ , the scattered wave is given by

$$W_s = \left\{ \frac{J_1(ka)}{H_1^{(2)}(ka)} H_0^{(2)}(kr) + \sum_{n=1}^{\infty} 2(-j)^n \frac{J_{n+1}(ka) - J_{n-1}(ka)}{H_{n+1}^{(2)}(ka) - H_{n-1}^{(2)}(ka)} H_n^{(2)}(kr) \right\} \cos n\theta, \quad (1)$$

where  $J_n$  are the Bessel functions of the first kind and order  $n$ ,  $H_n^{(2)}$  are the Hankel functions of the second kind and order  $n$ ,  $k$  the wave number, and  $a$  the cylindrical obstacle's radius.

For the numerical evaluation of Eq. (1), the first 30 coefficients were calculated: it was found that the higher coefficients have a negligible influence on the scattered field. In Fig. 1, the polar plots of the scattering field for different obstacle radii are presented. In this example, it is considered that the incident field propagates from the left to the right in an aluminium plate with 1 mm thickness at 1 MHz frequency. Under these conditions, it was considered that the A0 mode has exclusively out-of-plane displacement with a phase velocity is 2335 m/s and the wave number  $k$  is equal to 2690 m<sup>-1</sup>. The wave is received 140 mm away from the centre of the holes. As expected, the maximum of the scattering field is obtained in the direction of the incident wave and the greater the obstacle dimensions the greater the field value.

### 3. EXPERIMENTAL

#### 3.1. Experimental Setup

The experimental setup used in this work is schematically shown in Fig. 2. In the pitch-and-catch technique, a pair of immersion transducers are used: one as the transmitter and another as the receiver. In our experiments, two pairs of transducers (500 kHz and 1 MHz) were utilized. A Panametrics 5800 PR pulser/receiver (Olympus NDT, Waltham, MA, USA) excites the transmitter. After propagation on the plate, the ultrasonic signal is collected by the receiver, amplified, and filtered by the pulser/receiver. Then, in order to increase the signal-to-noise ratio, the signal is averaged by a digital oscilloscope, and finally transferred to a computer for further processing. Each transducer is connected to a rotating stage to control its angular inclination. By using the pulse-echo technique, a single transducer operates both as transmitter and receiver; the collected signal results from the reflection from the defect or obstacle existing in the plate. The use of

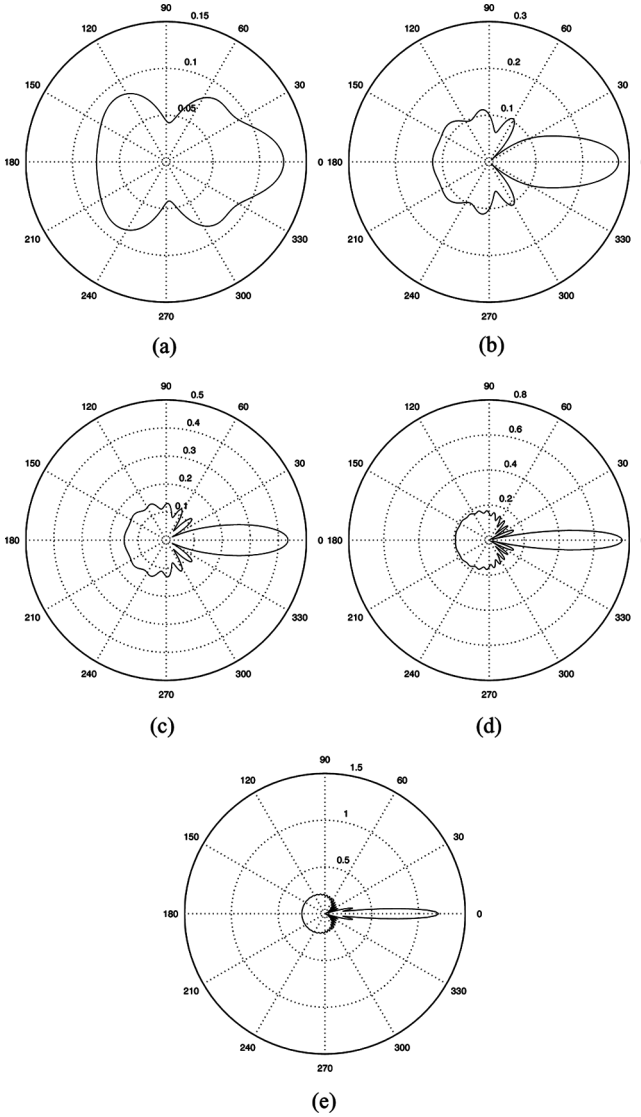


**FIGURE 1** Polar plots of the scattering field for different holes radius. The incident mode is  $A_0$  in an aluminium plate ( $fd = 1$  MHz.mm) and the receiver is 140 mm away from the centre of the holes: (a)  $ka = 5.4$ ; (b)  $ka = 10.8$ ; (c)  $ka = 16.2$ ; (d)  $ka = 26.9$ ; (e)  $ka = 43$ .

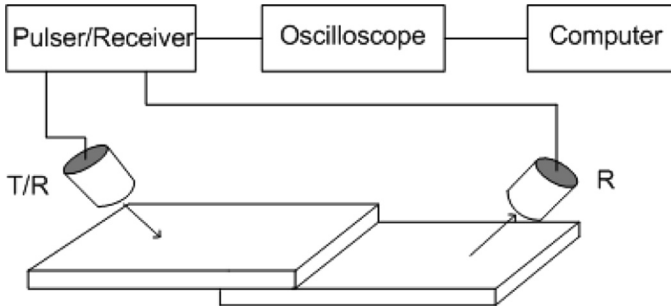


**FIGURE 2** Experimental setup.

an immersion method is due to the necessity to guarantee the same coupling between the transducers and the plate, allowing reproducible test conditions.

It is important to identify a particular propagation mode of the guided waves. Due to their dispersive behaviour, frequency domain techniques are demanded in order to get a correct velocity evaluation. The phase spectrum method is extensively used. In this method, the phase velocity is given by

$$C_p = \frac{2\pi fL}{\Delta\varphi}, \quad (2)$$

where  $f$  is the frequency and  $\Delta\varphi$  the difference in the phase spectrum of the two signals distant  $L$  from each other [31].

In Fig. 3, the theoretical dispersion curves of the fundamental propagation modes (A0 and S0) for an aluminium plate of 1 mm thickness obtained by using the transfer matrix technique together with an experimental one are presented. The latter was obtained by applying the pitch-and-catch technique and the phase spectrum method for two signals collected (in the receiver plate) 40 mm apart and using 500 kHz transducers oriented *via* the coincidence principle. It can be seen in Fig. 3 that the propagation mode is A0.

It is also important to analyse the displacement profiles of the propagation mode that was used. Figure 4 shows the displacement profiles for the A0 mode propagating in an aluminium plate 1 mm thick, at 500 kHz and 1 MHz. In both cases, it is possible to see that the out-of-plane displacement is dominant which allows the use, as an approximation, of the simplified model presented in Section 2.2.

By using the pitch-and-catch technique in a single plate, a chosen propagation mode is excited in the transmitter side of the plate, being



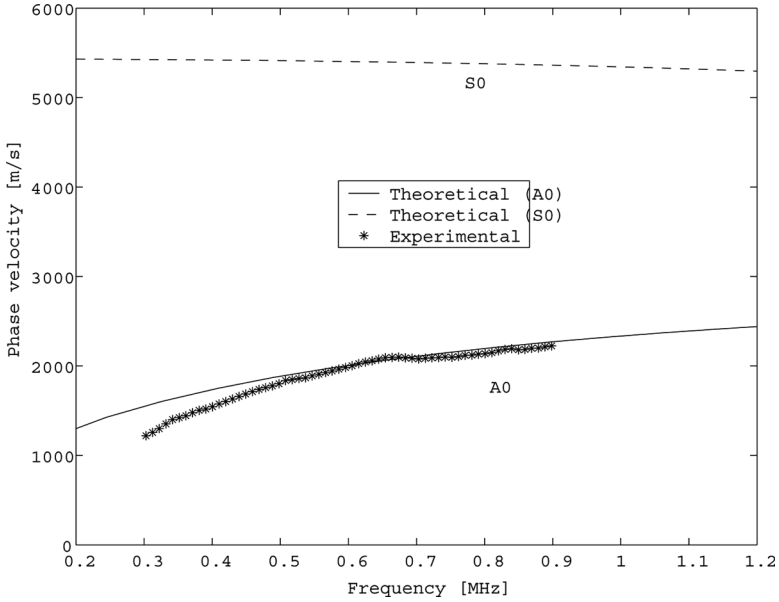


**FIGURE 3** Theoretical dispersion curves of the fundamental propagation modes A0 and S0, and the experimental one for an aluminium plate of 1 mm thickness.

the same mode collected at the other side (receiver). For the case of the lap joint analysed in this work, the required mode is excited in one side of the system (the transmitter plate) (Fig. 2), travels across the adhesive lap joint, and is received in the second plate (the receiver

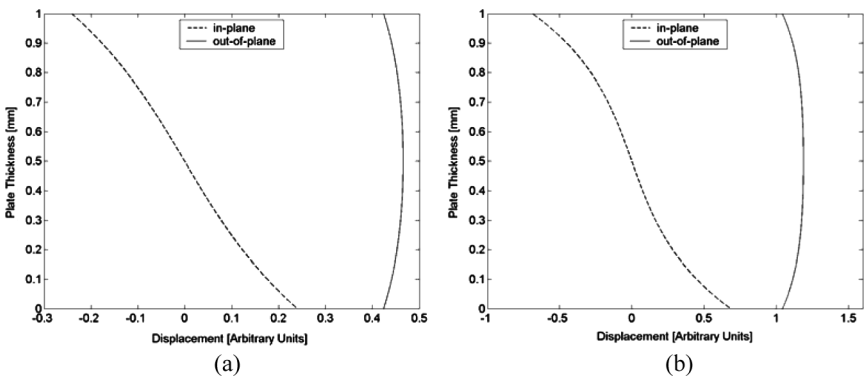


**FIGURE 4** Displacement profiles for A0 mode in 1 mm thickness aluminium plate: (a) 500 kHz; (b) 1 MHz.

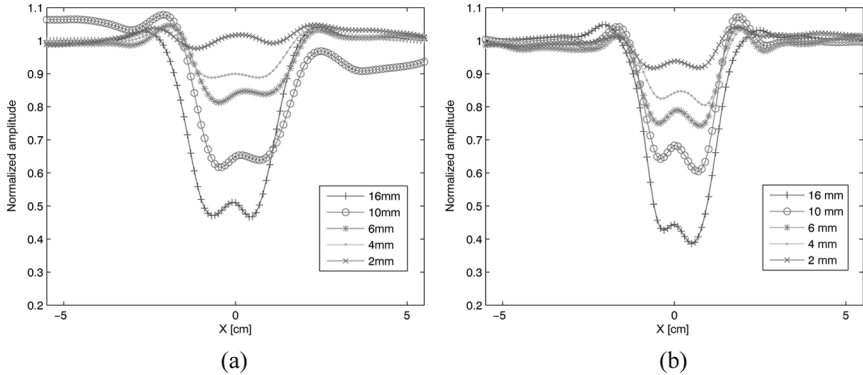


**FIGURE 5** Normalized amplitude measurements for different holes diameters as a function of the transducer's displacement: (a) 500 kHz; (b) 1 MHz.

plate). The wave in the transmitter plate is converted to other modes at the location where it first meets the adhesive layer. These new waves, which travel in the bonded region, are the natural modes of the three-layer system. At the end of the bonded region, further mode conversion takes place, giving rise to the original mode existing in the transmitter plate. These natural modes in the three-layer system are later analysed.

### 3.2. Inspection of Plates with Through-Holes

A set of preliminary tests was done on 1 mm thick and 20 cm width aluminium plates having through-holes with different diameters. In Fig. 5, the normalized amplitude of the signal as a function of the transducer's displacement obtained with the pitch-and-catch technique, at 500 kHz and 1 MHz, are presented. The transducers move rigidly and parallel to the sides of the plate; for  $x = 0$ , the transducers are aligned with the centre of the hole (Fig. 6). The distance between the transducers is 28 cm. For both the frequencies, it is possible to see a decrease in the received signal as the hole diameter enlarges, which is due to the increase of the shadow zone where there is no direct transmission. When the transducers are aligned with the centre of the holes ( $x = 0$ ), there is a local maximum that is related to the scattering effect. The lack of perfect symmetry around  $x = 0$  has to do not only with the imperfect parallelism in the experimental setup but also with the fact that the plates are not perfect planes, which is more difficult the thinner they are.

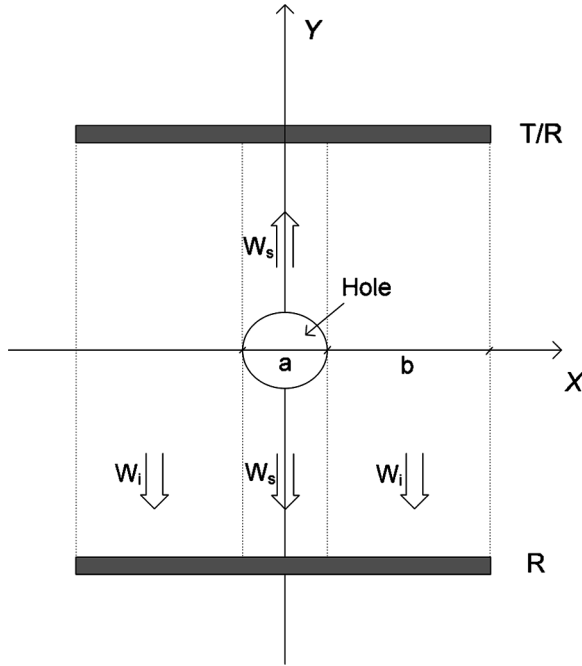


**FIGURE 6** Geometry of the problem.

From here on our analysis will be concerned with the case where  $x = 0$ , because it is the most interesting when trying to localize and classify voids in bond structures.

For the calculations, we assume that the amplitude at the receiver ( $A_R$ ) sums up the influence of the scattering field ( $W_s$ ) [Eq. (1)] and of the incident field ( $W_i$ ); obviously, the hole dimensions ( $a$ ) and the beam width, which is not obstructed by the hole ( $2b$ ) (Fig. 6), have to be taken into account. In our experimental setup, the scattering field ( $W_s$ ) originated by the holes is considered constant at the receiver, taking into consideration the transducer's diameter ( $D$ ) and the transducer-hole distance ( $r$ ). Indeed, the value of the angle seen by the borders of the transducer, for the case of the 500 kHz transducer which has a diameter of  $D = 20$  mm, is equal to  $\theta = 4^\circ$  [ $\theta = \tan^{-1}(D/2)/r = \tan^{-1}(10/140)$ ]. So, from Fig. 1, it can be seen that for angles lower than this value it is reasonable to consider the scattering field as almost constant for all hole dimensions. The direct incident field ( $W_i$ ) that propagates in the plate without any influence of the obstacles is also considered constant.

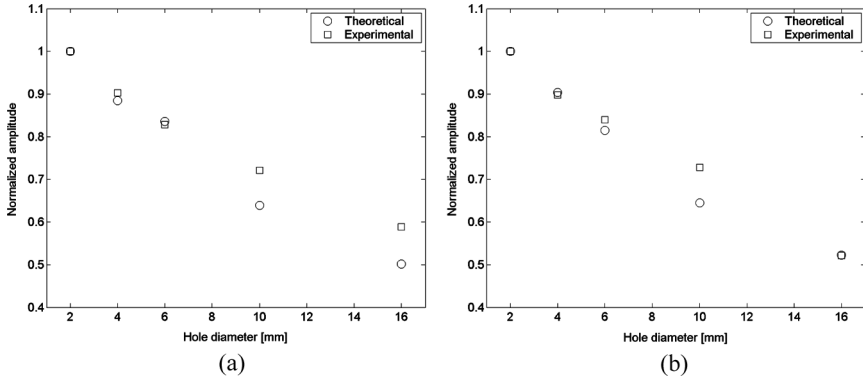


**FIGURE 7** Theoretical and experimental normalized amplitudes for different hole diameters obtained using pitch-and-catch technique: (a) 500 kHz; (b) 1 MHz.

The receiving signal is then given approximately by

$$A_R = W_i 2b + W_s a. \quad (3)$$

In Fig. 7, the theoretical and experimental amplitudes as functions of the hole diameters at 500 kHz and 1 MHz are presented. To allow the comparison of the normalized amplitudes of the theoretical and experimental fields, it was necessary to adopt an arbitrary unit as a reference. This was done by setting both the theoretical and experimental values for the 2 mm hole diameter equal to one (1). The bigger the hole diameter the smaller the amplitude, as Eq. (2) explains. Despite the increase of  $W_s$  with  $a$ , as Fig. 1 shows, the decreasing of  $b$  implies the decrease of the receiving field, in such a way that a decay of the total receiving signal is obtained.

In the pulse-echo technique, the collected signal is given by the reflection from the existing hole in the plate, which is the backscattering signal. In Fig. 8, the theoretical and experimental amplitudes, normalized in the same way as in Fig. 7, *versus* hole diameters obtained with the transducer aligned with the centres of the holes for 500 kHz and 1 MHz are presented. In this case, there is an increase of the collected signal with the increase of the dimensions of the holes, as can be seen in Fig. 1, in agreement with other studies [30].

Quantitative differences between pitch-and-catch and pulse-echo techniques are due to the approximations considered in the analytical model, namely, to the fact that the incident wave was considered exclusively as an out-of-plane displacement.

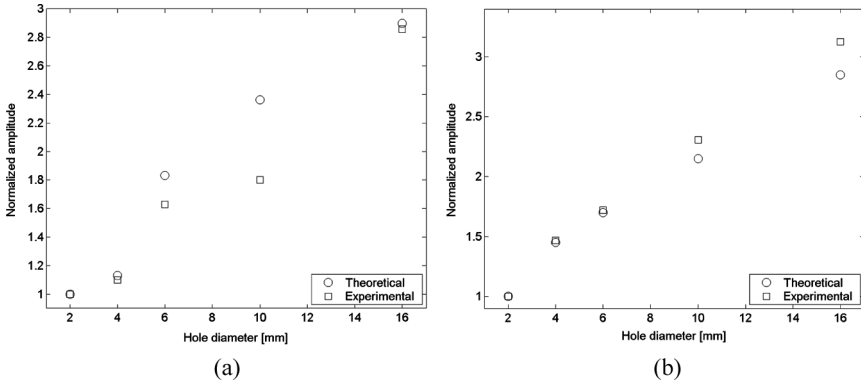


**FIGURE 8** Theoretical and experimental normalized amplitudes for different holes diameters obtained using pulse-echo technique: (a) 500 kHz; (b) 1 MHz.

### 3.3. Inspection of Bonded Lap Joints

To study the scattering effects of defects in the bond line, samples with different defect dimensions were produced. The sample fabrication process, already referred to by the author in a previous work [22], produces artificial defects with good reproducibility and consists of drilling a cavity with a diameter of the order of the adhesive thickness in one of the plates. Afterwards, this region is covered with a sticky tape to avoid adhesive diffusion. Finally, this plate is bonded together with the second plate by means of an epoxy adhesive (Araldite 2014, Vantico, Duxford, Cambridge, UK). In practice the cavity, without any adhesive in its interior, behaves like a void. The aluminium plates were 20 cm in length and the bonding region is all along the width (20 cm) and 6 cm in length. The epoxy adhesive used is of 0.15 mm thickness obtained through a uniform pressure of  $0.1 \text{ Kg/m}^2$ . The adhesive was then cured according to the manufacturer's instructions at room temperature ( $25^\circ\text{C}$ ) for 24 h.

To validate this kind of sample preparation, some adhesively bonded lap joints with real defects were produced in the classical way. That consists of leaving a circular area at the bonding zone in one of the plates without adhesive and then submitting the joint to a uniform stress. With this method, it is very difficult to guarantee that the final joint has the same disbonded area at the same conditions. After several attempts, some lap joints with circular disbonded areas with 4, 6, and 10 mm diameter were obtained. This was confirmed by using ultrasonic C-scan images.

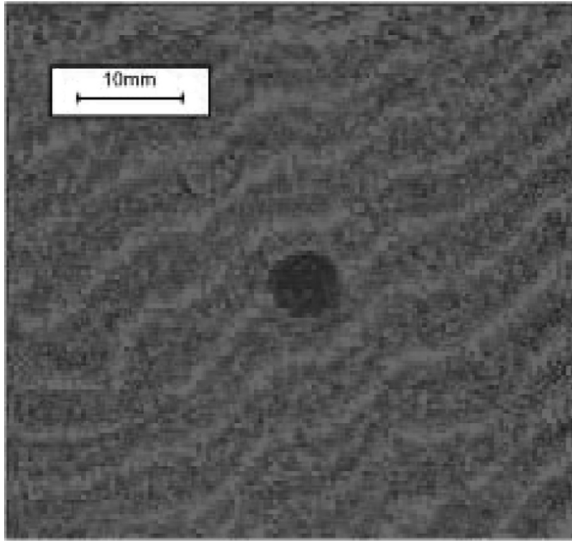


**FIGURE 9** Ultrasonic C-scan image of a circular artificial defect 6 mm in diameter.

In Fig. 9, an example of an artificial circular defect 6 mm in diameter is presented. It was experimentally verified that the scattering effects of this kind of artificial and real defects with the same dimensions are approximately the same, which confirms that the technique is adequate to produce artificial defects in bonded lap joints.

The methodology used for the inspection of the lap joints with the artificial defects was the same as that used for the inspection of the plates with through holes. Applying the pitch-and-catch technique with 1 Mhz transducers, we verified an increase in the received signal with an increase in the defect's dimensions, when the transducers are aligned with the centre of the defects. This phenomenon can be explained (Fig. 10) in a way similar to the scattering by the holes. In this case, the shadow zone does not exist because, in the presence of the defect, the system can be seen as a set of two isolated plates where the propagation still exists: in this way, the incident wave that travels in the two isolated plates is added to the scattering effects produced by the defect. In Eq. (2) the first term ( $W_i 2b$ ) is now constant and the second term ( $W_s a$ ), related to the scattering, grows with the defect dimensions.

In Fig. 11, theoretical and experimental results normalized in the same way as in Figs. 7 and 8 (the reference defect dimension is now

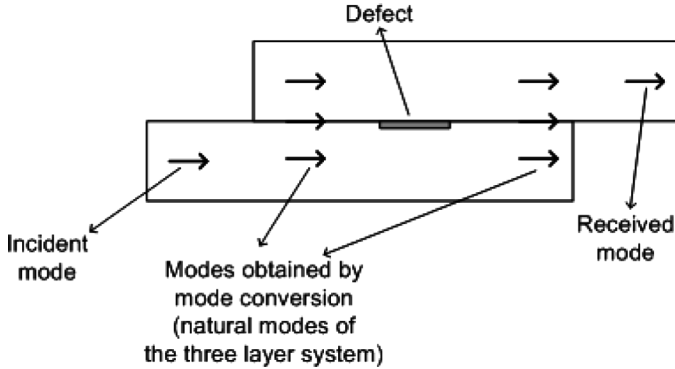


**FIGURE 10** Existing modes in single layers and in three Layer system.

3 mm) for 500 kHz and 1 MHz are presented. For 1 MHz frequency, it is possible to see a reasonable agreement. Discrepancies with a value around 5% are related to the simplified model used in this approach, especially due to the fact that the considered incident wave does not suffer exclusively out-of-plane displacement. For 500 kHz, larger discrepancies were found. In this case, an additional reason for these discrepancies can be related to the increase of the transducer's diameter (from 10 to 20 mm) that, consequently, gives rise to the increase of beam width and of the direct incident field, that masks the scattering field.

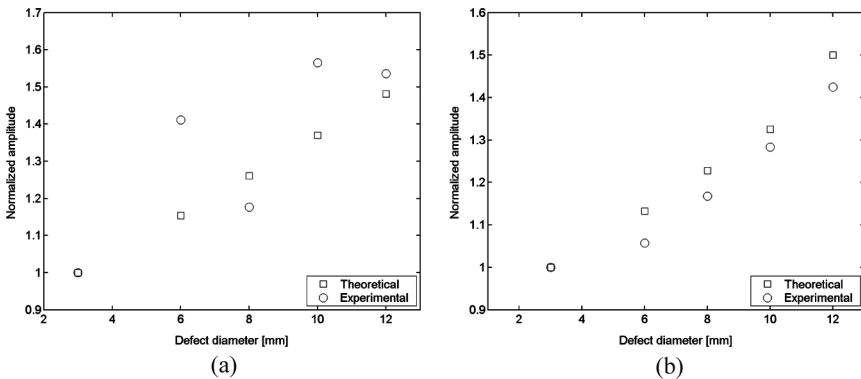


**FIGURE 11** Theoretical and experimental normalized amplitudes for different defect diameters obtained using pitch-and-catch technique: (a) 500 kHz; (b) 1 MHz.

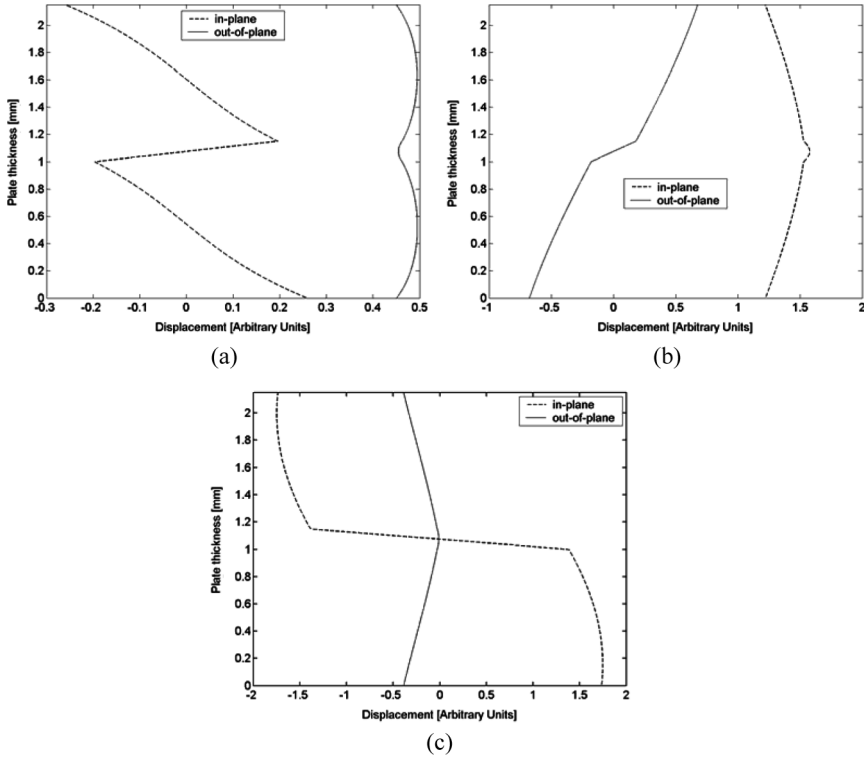


**FIGURE 12** Displacement profiles for the existing modes in the bonding zone for 500 kHz: (a) A0; (b) S0; (c) A1.

Another important reason for discrepancies between experimental and theoretical results is the existence of several propagation modes in the bonding zone, different for 1 MHz and 500 kHz, which causes different scattering effects. In Figs. 12 and 13 the displacement profiles of these modes are presented. For 500 KHz there are three modes (A0, S0, and A1) and for 1 MHz four modes (A0, S0, A1, and S1). Theoretically [32], it is expected that to excite a certain mode in the bonded zone, the mode shape in the bottom plate of the bonded zone should be similar to the mode shape of a single plate. Comparing the displacements in single plates (Fig. 4) and in bonded plates (Figs. 12 and 13) we can see that, for 500 kHz, the A0 mode has a similar shape in both situations considered, while for 1 MHz there are two modes with similar shape of a simple plate: A0 and S0. These are the dominant modes in the bonding zone.



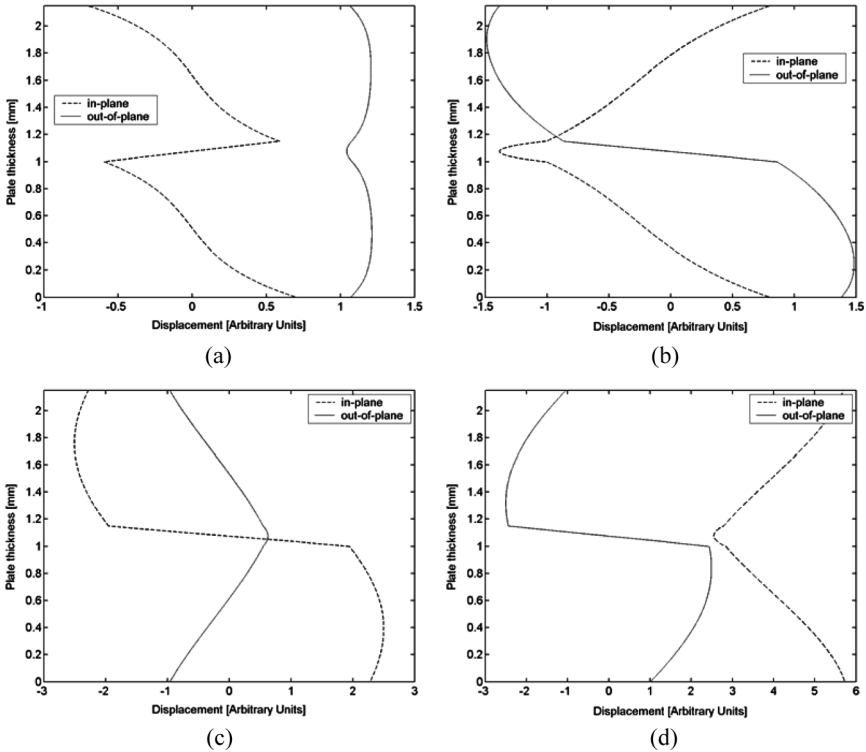


**FIGURE 13** Displacement profiles for the existing modes in the bonding zone for 1 MHz: (a) A0; (b) S0; (c) A1; (d) S1.

Despite the simplifications of the presented model, we can say that it can be used when a rough estimation of defect dimensions in bonded lap joints is needed. For more accurate analysis a more detailed model should be used.

With the pulse-echo technique, it was not possible to measure the scattering signals from the defects in the bond. This is due to the fact that the tail of the excitation signal overlaps the reflected signal, which has very low amplitude. This low amplitude is related to the leaking of energy to the fluid (attenuation) and to the fact that the scattering effects in the incident field direction are higher than the backscattering (opposite direction of the incident field), as we can see in Fig. 1.

#### 4. CONCLUSIONS

Conventional ultrasonic non-destructive evaluation of adhesively bonded joints is based, essentially, on point by point techniques. If an

accurate measure of defect dimensions is needed, C-scan can be used in the usual way with good results. The major limitation of this technique is the fact that is very time-consuming because the transducer needs to scan every point of the structure to be tested.

The use of ultrasonic guided waves is potentially a very attractive solution, giving rise to a considerable time saving when tests of large structures are demanded, since they can be excited at one point and propagated over considerable distances with low attenuation. With the pitch-and-catch technique, information about the line between transmitter and receiver can be obtained. In the case of the pulse-echo technique, the information about the line between transmitter and target can be obtained.

To analyse the scattering effects, a set of preliminary tests was done on aluminium plates with through holes with different diameters. The results using both the pitch-and-catch and the pulse-echo techniques are explained by a simplified theoretical model, considering the incident wave mainly with out-of-plane displacement.

To analyse the scattering effects of defects in the bond line of lap joints, several samples with different defects diameters were produced. The dimensions of these artificial defects were successfully confirmed with the help of ultrasonic C-scan images. As in the case of the hole analysis, the transducers were again aligned with the centres of the defects and the received amplitude was measured. Using the pulse-echo technique, it was not possible to form any conclusions about defect detection. The reasons why are related to: a) the tail of the exciting signal masking the potential backscattering received signal, which is lower than scattering in the incident field direction and b) the high attenuation due to the energy leak to the fluid.

With the pitch-and-catch technique, the results obtained compared with the theoretical ones are in reasonable agreement for 1 MHz transducers; differences are less than 5% lower. For 500 kHz the discrepancies are much higher. This can be understood based on the limitations of the model, which considers the displacements exclusively out-of-plane and do not take into account the non-dominant modes existing in the bonding region. So, it can be said that this technique can be used to roughly evaluate defect dimensions in a lap joint. For more accurate analysis, a more detailed model must be developed.

## REFERENCES

- [1] Adams, R. D. and Drinkwater, B. W., *NDT&E* **30**, 93–98 (1997).
- [2] Guyott, C., Cawley, P., and Adams, R., *Adhesion* **10**, 96–112 (1986).
- [3] Goglio, A. and Rosseto, M., *NDT&E* **32** 323–331 (1999).

- [4] Nieminen, A. O. K. and Koenig, J. L., *Int. J. of Adhesion and Adhesives* **11**, 5–10 (1991).
- [5] Windels, F. and Leroy, O., *Ultrasonics*, **40** 171–176 (2002).
- [6] Schindel, D. W., Forsyth, D. S., Hutchins, D. A., and Fahr, A., *Ultrasonics* **35**, 1–6 (1997).
- [7] Brotherhood, C. J., Drinkwater, B. W., and Dixon, S., *Ultrasonics* **41**, 521–529 (1997).
- [8] Guyott, C. and Cawley, P., *NDT International* **21**, 233–240 (1991).
- [9] Robinson, A. M., Drinkwater, B. W., and Allin, J., *NDT&E International* **36**, 27–36 (2003).
- [10] Allin, J. M., Cawley, P., and Lowe, M. J. S., *NDT&E International* **36**, 503–514 (2003).
- [11] Rienks, K. J., Fokker Bond Tester Model 70: Operation Manual, Report R-1498 (Royal Netherlands Aircraft Factories Fokker, Amsterdam, 1972).
- [12] Rokhlin, S., *J. Acoust. Soc. Am.* **89**, 2758–2965 (1991).
- [13] Heller, K., Jacobs, L. J., and Qu, J., *NDT&E International* **33**, 555–563 (2000).
- [14] Singher, L., *Ultrasonics* **35**, 305–315 (1997).
- [15] Chona, R., Suh, C. S., and Rabroker, G. A., *Opt. Lasers Eng.* **40**, 371–378 (2003).
- [16] Kundu, T., Maji, A., Ghosh, T., and Maslov, K., *Ultrasonics* **35**, 573–580 (1998).
- [17] Seifried, R., Jacobs, L. J., and Qu, J., *NDT&E International* **35**, 317–328 (2002).
- [18] Vasudeva, R. Y. and Sudheer, G., *Int. J. Solids Struct.* **39**, 559–569 (2002).
- [19] Lowe, M. J. S., Challis, R. E., and Chan, C. W., *J. Acoust. Soc. Am.* **107**, 1333–1345 (2000).
- [20] Scalea, F. L., Rizzo, P., and Marzani, A., *J. Acoust. Soc. Am.* **115**, 146–156 (2004).
- [21] Tood, C. and Challis, R., *IEEE Trans Ultrason Ferrelec Freq Control* **46**(1), 167–181 (1999).
- [22] Santos, M. and Perdigão, J., *NDT&E International* **38**, 561–568 (2005).
- [23] Lowe, M. J. S., *IEEE Trans Ultrason Ferrelec Freq Control* **42**, 525–542 (1995).
- [24] Hosten, B. and Castaings, M., *J. Acoust. Soc. Am.* **94**, 1488–1495 (1993).
- [25] Nagy, P. and Adler, L., *J. Appl. Phys.* **66**(10), 4658–4663 (1989).
- [26] Norris, A. and Vemula, C., *J. Sound and Vib.* **181**(1), 115–125 (1995).
- [27] Chang, Z. and Mal, A., *Mechanics of Materials* **31**, 197–204 (1999).
- [28] Wang, X. and Ying, C., *J. Acoust. Soc. Am.* **110**(4), 1752–1763 (2001).
- [29] Fromme, P. and Sayir, M., *J. Acoust. Soc. Am.* **111**(3), 1165–1170 (2002).
- [30] Diligent, O., Grahn, T., Bostrom, A., Cawley, P., and Lowe, M., *J. Acoust. Soc. Am.* **112**(6), 2589–2601 (2002).
- [31] Santos, M., Ferreira, A., and Perdigão, J., *Mater. Eval.* **64**(4), 433–439 (2004).
- [32] Auld, B. A., *Acoustics Fields and Waves in Solids* (Krieger, Malabar, FL, 1990), 2nd ed.